Talanta 85 (2011) 1980–1985

Contents lists available at ScienceDirect

Talanta

journal homepage: www.elsevier.com/locate/talanta

One step electrochemically deposited nanocomposite film of chitosan–carbon nanotubes–gold nanoparticles for carcinoembryonic antigen immunosensor application

Xia Gao, Yiming Zhang, Qi Wu, Huan Chen, Zhichun Chen, Xianfu Lin*

Department of Chemistry, Zhejiang University, Hangzhou 310027, PR China

ARTICLE INFO

Article history:
Received 28 April 2011
Received in revised form 4 July 2011
Accepted 7 July 2011
Available online 18 July 2011

Keywords:
Immunosensor
One-step electrochemical deposition
Chitosan
Carbon nanotubes
Gold nanoparticles
CEA

ABSTRACT

A simple and controllable one-step electrodeposition method for the preparation of a chitosan–carbon nanotubes–gold nanoparticles (CS–CNTs–GNPs) nanocomposite film was used to fabricate an immunosensor for detection of carcinoembryonic antigen (CEA). The porous three-dimensional CS–CNTs–GNPs nanocomposite film, which offered a large specific surface area for immobilization of antibodies, exhibited improved conductivity, high stability and good biocompatibility. The morphology of the formed nanocomposite film was investigated by scanning electron microscopy (SEM), and the electrochemical behaviors of the immunosensor were characterized by electrochemical impedance spectroscopy (EIS) and cyclic voltammetry (CV). Under the optimal conditions, the proposed immunosensor could detect CEA in two linear ranges from 0.1 to 2.0 ng mL^{-1} and from 2.0 to 200.0 ng mL^{-1}, with a detection limit of 0.04 ng mL^{-1}. The immunosensor based on CS–CNTs–GNPs nanocomposite film as the antibody immobilization matrix could exhibit good sensitivity, stability, and reproducibility for the determination of CEA.

1. Introduction

Immunoassay techniques, which are based on the highly specific molecular recognition of antigens by antibodies, have become the main analytical methods in clinical, biochemical, pharmaceutical and environmental fields [1]. In recent years, electrochemical immunosensors have attracted extensive interest because of the advantages such as high sensitivity, a relatively low detection limit, fast analysis and low cost of both the sensors and the instrumentation [2–4].

The effective immobilization of biomolecules is a key point in fabrication of immunosensors. An ideal immobilization process should be simple and maintain the bioactivity and stability of the biomolecules [5]. As one of the most promising matrix for biomolecules immobilization, chitosan (CS), a polysaccharide derived by deacetylation of chitin, has become the subject of intense investigation due to its cheapness, excellent film-forming ability, high water permeability, good adhesion, nontoxicity and remarkable biocompatibility [6–9]. For example, Tan et al. prepared an amperometric immunosensor for rapid determination of α-1-fetoprotein based on α-1-fetoprotein antibody/TiO_2 nanoparticles/chitosan film [10]. Lin et al. [11] developed a sensitive immunosensor by immobilizing α-fetoprotein antigen onto the glassy carbon electrode modified by a gold nanoparticles and carbon nanotubes doped chitosan film. However, CS was usually manually cast on the surface of electrodes to form films with uncontrollable thickness, which might lead to poor repeatability and reproducibility.

Electrochemical deposition has been applied as a simple and controllable method to obtain CS films which tightly attached to the electrode [12–14]. CS is a pH shift polymer with a p*K*a of about 6.3 due to its primary amino groups [15,16]. At pH below the p*K*a, CS is a water-soluble, cationic polyelectrolyte because most of the amino groups are protonated. At pH above the p*K*a, the amino groups become deprotonated, and CS loses its charges and becomes insoluble. When the electrodeposition is performed at reducing potentials, H^+ in the solution is reduced to H_2 at the cathode, and pH near the cathode surface gradually increases. The locally generated H^+ gradient results in a change in solubility of CS and the formation of a CS film [17,18]. In addition, many other substances such as enzymes [19], gold nanoparticles [20,21], and carbon nanotubes [22] can be incorporated into the CS film during the electrodeposition process. Several literatures have reported the fabrication of immunosensors based on electrochemically deposited CS films. Qiu's group constructed a label-free immunosensor with a conductive redox chitosan–ferrocene film and gold nanoparticles [23]. To improve the conductivity of the prepared film, multiwalled carbon nanotubes were further introduced

* Corresponding author. Fax: +86 571 87951895.
E-mail address: llc123@zju.edu.cn (X. Lin).

0039-9140/$ – see front matter © 2011 Elsevier B.V. All rights reserved.
doi:10.1016/j.talanta.2011.07.012

into the CS–Fc composite [24]. Yuan's group developed label-free immunosensors based on CS films that covalently bounded with thionine, employing gold nanoparticles for immobilization of antibodies [25–27]. These immunosensors based on electrochemically deposited CS films were controllable and reproducible.

In this work, a new antibody immobilization strategy based on electrochemically deposited nanocomposite film of chitosan–carbon nanotubes–gold nanoparticles (CS–CNTs–GNPs) was used to develop an immunosensor. The stable CS–CNTs–GNPs nanocomposite film was formed on the electrode surface by one-step electrodeposition method. Carbon nanotubes (CNTs), with high chemical stability and mechanical strength, could improve the conductivity of the prepared nanocomposite film. Gold nanoparticles (GNPs) could also effectively facilitate the electron transfer due to their good conductivity. Moreover, the porous three-dimensional CS film incorporated with CNTs and GNPs could provide a high accessible surface area and a good biocompatible microenvironment for immobilization of antibodies. Here, carcinoembryonic antigen (CEA), an acidic glycoprotein with a molecular weight of approximately 200 kDa, which is one of the most important tumor markers for clinical diagnoses [28,29], was used as a model. The carcinoembryonic antibody (anti-CEA) was immobilized on the electrode modified with CS–CNTs–GNPs nanocomposite film. Such approach was direct and facile without complicated and time-consuming manual process. The prepared immunosensor for detection of CEA showed high sensitivity, low detection limit and long-term stability.

2. Experimental

2.1. Reagents

CEA and anti-CEA were purchased from Keyuezhongkai Biotech Co., Ltd. (Beijing, China) and stored at 4 °C. Chitosan (CS, MW 480,000, 92% deacetylation) was obtained from Golden-shell Biochemical Co., Ltd. (Zhejiang, China). CS aqueous solution (0.5 wt%, pH 5.0) was prepared according to the previously reported procedure [13,30]. The multiwalled carbon nanotubes (MWCNTs, 95%,) were purchased from Nanotech. Port. Co., Ltd. (Shenzhen, China). Prior to use, MWCNTs were treated in order to introduce carboxylic acid groups according to the reference [31]. Hydrogen tetrachloroaurate ($HAuCl_4{\cdot}4H_2O$) and bovine serum albumin (BSA, 98%) were obtained from Sinopharm Chemical Reagent Co., Ltd. (Shanghai, China). Gold nanoparticles (GNPs) were prepared according to the reported method by boiling $HAuC1_4$ aqueous solution with trisodium citrate [32] and were stored in a brown bottle at 4 °C. The average diameter of the prepared GNPs was about 16 nm. CEA enzyme-linked immunosorbent assay (ELISA) kits were purchased from Autobio Co., Ltd. (Zhengzhou, China). All other chemicals were of analytical grade and used without pretreatments. Double distilled water was used throughout the work. Phosphate buffer solutions (PBS, 0.02 M) at various pH values were prepared by mixing the stock standard solutions of NaH_2PO_4 and Na_2HPO_4.

2.2. Apparatus

Electrochemical measurements were performed on a CHI 650C electrochemical workstation (Shanghai CH Instrument Company, China). A conventional three-electrode electrochemical cell was used with a platinum disk electrode as the auxiliary electrode, a saturated calomel electrode (SCE) as the reference electrode and a modified glassy carbon electrode (GCE, $\Phi = 4$ mm) as the working electrode. Scanning electron microscopy (SEM) images were obtained at 5.0 kV on a scanning electron microscope (Zeiss Ultra 55). The average diameter of gold nanoparticles was estimated by transmission electron microscopy (TEM) (JEM-1200EX).

2.3. Preparation of CS–CNTs–GNPs nanocomposite solution

CS–CNTs–GNPs nanocomposite solution was prepared according to the method reported previously [33] with a slight modification. Briefly, 1.5 mL carboxylated MWCNTs dispersion ($1.0\ mg\ mL^{-1}$) was added into 3 mL of the prepared CS solution (0.5 wt%, pH 5.0) with 20 min ultrasonication to obtain a homogeneous suspension. Subsequently, the gold colloidal was mixed with the black suspension and the mixture was ultrasonicated for 10 min to obtain the CS–CNTs–GNPs nanocomposite.

2.4. Fabrication of the immunosensor

Before modification, the bare glassy carbon electrode was successively polished with 1.0, 0.3 and 0.05 μm alumina slurry and rinsed with double distilled water. The electrode was successively sonicated in double distilled water, ethanol and double distilled water for 5 min, and then allowed to dry at room temperature. The polished GCE was dipped into the as-prepared CS–CNTs–GNPs nanocomposite solution and the electrodeposition was performed by applying a constant voltage of −1.5 V for 3 min. After electrodeposition, the modified electrode (CS–CNTs–GNPs/GCE) was removed from the solution and rinsed with double distilled water, then dried in air at room temperature. Subsequently, 5 μL of anti-CEA solution was dropped onto the surface of the modified electrode at 4 °C for 12 h. Finally, the modified electrode was incubated in 0.2% BSA for 2 h in order to block possible remaining active sites and avoid the non-specific adsorption. The finished immunosensor was stored at 4 °C when not in use. The fabricated procedure of the immunosensor was shown in Fig. 1.

2.5. Electrochemical measurements

Electrochemical measurements were done in a conventional electrochemical cell at the room temperature of 25 °C. Electrochemical impedance spectroscopy measurements were carried out in 0.02 M PBS (pH 6.5) containing 5.0 mM $K_3[Fe(CN)_6]/K_4[Fe(CN)_6]$ (1:1) mixture and 0.1 M KCl with the frequencies ranging from 10^4 to 10^{-1} Hz. Cyclic voltammograms (CVs) were performed in 0.02 M PBS (pH 6.5) containing 5.0 mM $K_3[Fe(CN)_6]/K_4[Fe(CN)_6]$ (1:1) mixture and 0.1 M KCl from 0.6 to −0.2 V (versus SCE) at a scan rate of $50\ mV\ s^{-1}$. The detection was based on the change of reduction current response (ΔI) before and after the immunoreaction. When antigens had bound with the antibodies immobilized on the electrode, the antigen–antibody complexes coating on the surface of the electrode inhibited the electron transfer. Therefore, the change of peak current response increased directly proportional to the concentration of antigen after the immunoreaction [34]. The immunoreaction was performed by incubating the immunosensor in 0.02 M PBS (pH 6.5) containing various concentrations of CEA for 20 min at the room temperature of 25 °C and then electrochemical experiments were performed.

3. Results and discussion

3.1. Morphology characterization of the CS–CNTs–GNPs nanocomposite film

CS is a unique polymer which has pH-dependent electrostatic properties and is positively charged in acidic media [14–16]. The mechanism for CS deposition had been studied and interpreted as the formation of pH gradient near the cathode surface due to the

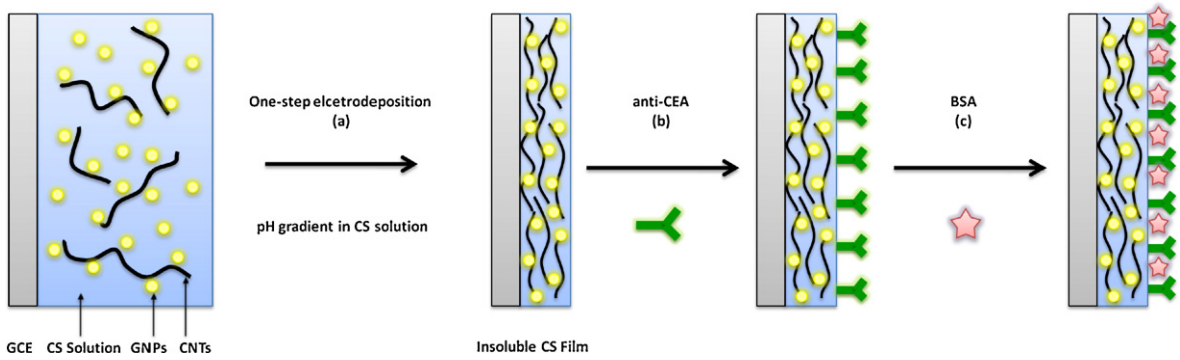

Fig. 1. Schematic illustration of the fabrication procedure of the immunosensor.

reduction of water [17,18]. At a constant electrodeposition potential, H^+ in the solution was electrochemically reduced to H_2 at the cathode, gradually increasing the local pH near the cathode surface. When pH was higher than the pK_a of CS (about 6.3), CS became insoluble and the CS entrapped CNT and GNPs would deposit onto the cathode surface as a result. The morphologies of CS–CNTs and CS–CNTs–GNPs nanocomposite films were investigated by SEM, as shown in Fig. 2. It was found that the CS–CNTs nanocomposite film exhibited a highly porous surface with a three-dimensional structure and many wire-like CNTs were distributed in the film (Fig. 2A). For the CS–CNTs–GNPs nanocomposite film (Fig. 2B), GNPs were uniformly dispersed in the film without obvious aggregation, suggesting that a nanocomposite film consisting of CS entrapped CNT and GNPs was formed through one-step electrodeposition process. The three-dimensional structure of the CS–CNTs–GNPs nanocomposite film could provide a favorable microenvironment for immobilization of antibodies. In addition, the entrapped CNTs and GNPs could provide a conductive pathway of electron-transfer.

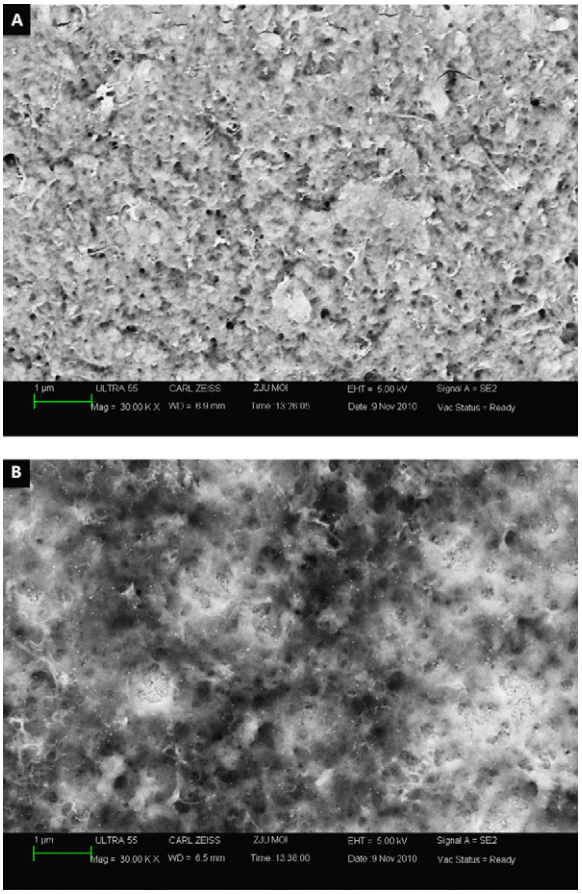

Fig. 2. SEM images of (A) CS–CNTs flim, (B) CS–CNTs–GNPs film.

3.2. Electrochemical characterization of the immunosensor

Electrochemical impedance spectroscopy (EIS) has been used to study the interface properties of modified electrodes [35]. In the EIS, the linear part at the low frequencies and the semicircle portion at the high frequencies correspond to the diffusion-limited process and the electron transfer-limited process, respectively. The semicircle diameter equals to the electron transfer resistance (R_{et}). Fig. 3 exhibited the EIS of the modified electrodes. It was observed that the EIS of the bare GCE displayed an almost straight line (Fig. 3a), indicating a diffusion-limited process. After deposition of a CS film, the R_{et} increased apparently and was estimated to be 433 Ω (Fig. 3b), which indicated the successful formation of CS film hindering the electron transfer of the electrochemical probe. When CS–CNTs was electrodeposited on the electrode surface, the value of R_{et} decreased to 155 Ω (Fig. 3c), implying that the incorporation of CNTs greatly facilitated the electron transfer. For the film of CS–CNTs–GNPs (Fig. 3d), the R_{et} further decreased to 34 Ω due to the increased conductivity, which proved that GNPs were favorable for the electron transfer. Subsequently, when anti-CEA was immobilized onto the modified electrode, the R_{et} increased obviously and was estimated to be 150 Ω (curve a of inset in Fig. 3). The result was ascribed to the nonconductive properties of anti-CEA which

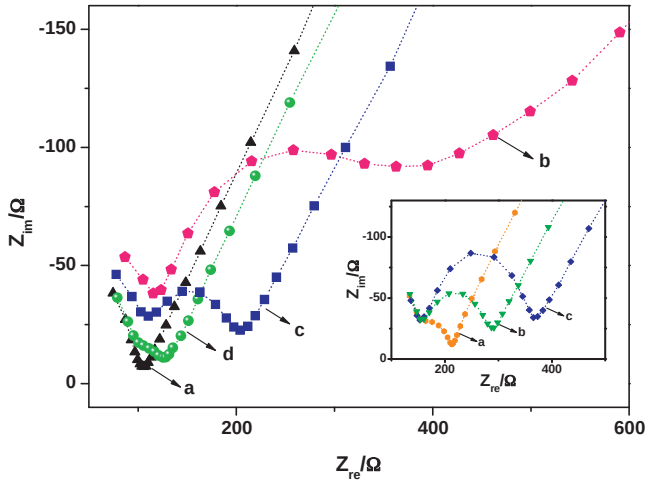

Fig. 3. EIS of different modified electrodes measured in 5.0 mM $[Fe(CN)_6]^{4-/3-}$ containing 0.1 M KCl (pH 6.5): (a) bare GCE; (b) CS/GCE; (c) CS–CNTs/GCE; (d) CS–CNTs–GNPs/GCE. The inset shows the EIS of (a) anti-CEA/CS–CNTs–GNPs/GCE; (b) BSA/anti-CEA/CS–CNTs–GNPs/GCE; (c) CEA/BSA/anti-CEA/CS–CNTs–GNPs/GCE.

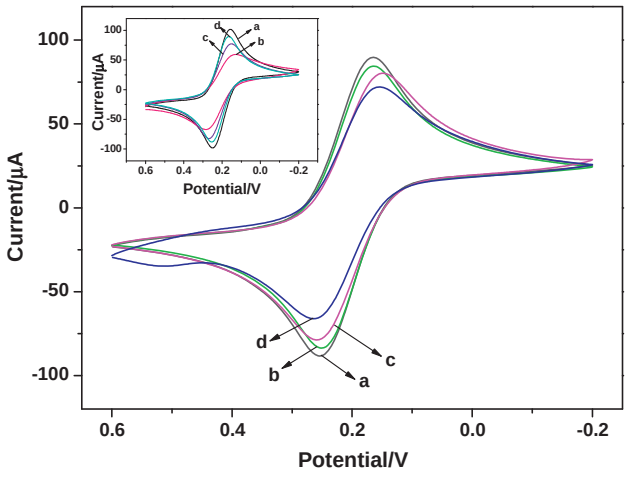

Fig. 4. CVs of different modified electrodes measured in 5.0 mM $[Fe(CN)_6]^{4-/3-}$ containing 0.1 M KCl (pH 6.5): (a) CS–CNTs–GNPs/GCE; (b) anti-CEA/CS–CNTs–GNPs/GCE; (c) BSA/anti-CEA/CS–CNTs–GNPs/GCE; (d) CEA/BSA/anti-CEA/CS–CNTs–GNPs/GCE. The inset shows the CVs of (a) bare GCE; (b) CS/GCE; (c) CS–CNTs/GCE; (d) CS–CNTs–GNPs/GCE.

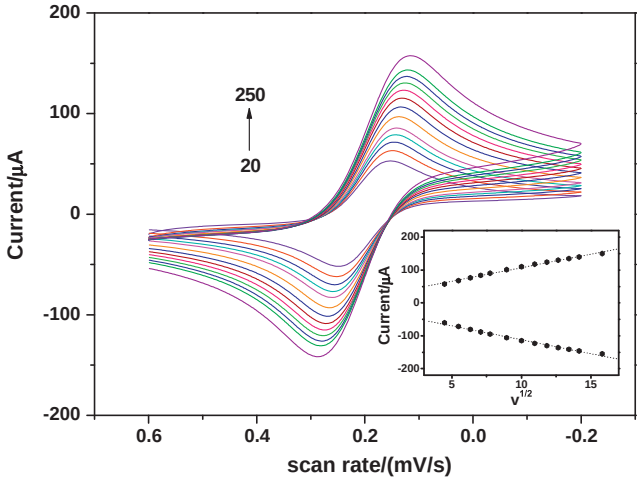

Fig. 5. CVs of the modified immunosensor at various scan rates in 5.0 mM $[Fe(CN)_6]^{4-/3-}$ containing 0.1 M KCl (pH 6.5). The inset shows the dependence of redox peak currents on the square root of scan rates.

acted as an inert electron layer and blocked the electron transfer. Similarly, the R_{et} also increased when BSA was used to block non-specific sites and was estimated to be 189 Ω (curve b of inset in Fig. 3). After the immunosensor was incubated with CEA antigen, the R_{et} further increased to 251 Ω (curve c of inset in Fig. 3), indicating that the formation of hydrophobic immunocomplex layer hindered the electron transfer.

Fig. 4 showed the cyclic voltammograms (CVs) of different modified electrodes. The redox-label $[Fe(CN)_6]^{4-/3-}$ revealed a reversible CV at the bare GCE (curve a of inset in Fig. 4). After deposition of a CS film, the peak current decreased obviously due to the CS film hindering the electron transfer (curve b of inset in Fig. 4). When CS–CNTs was electrodeposited on the electrode surface, the peak current was larger than that of CS film (curve c of inset in Fig. 4), which indicated that the CNTs improved the conductivity. For the film of CS–CNTs–GNPs (curve d of inset in Fig. 4), the peak current further increased, implying that the GNPs facilitated the electron transfer. However, the peak current decreased after anti-CEA was immobilized onto the modified electrode surface (Fig. 4b), which suggested that the big protein molecules hindered the electron transfer, in agreement with the results of EIS. A further decrease of the peak current was observed when BSA was employed to block non-specific sites (Fig. 4c). After the immunosensor was incubated with CEA antigen, the peak current decreased due to the immunocomplex blocking the tunnel for mass and electron transfer (Fig. 4d).

The CVs of the prepared immunosensor at different scan rates were shown in Fig. 5. It could be observed that the potentials and peak currents were dependent on the scan rate. Both the anodic and cathodic peak current were directly proportional to the square root of scan rates in the range of 20–250 mV s^{-1} (shown in the inset of Fig. 5), suggesting a diffusion controllable redox process. Thus, the scan rate chosen for the CVs was 50 mV s^{-1}, which was in the range of 20–250 mV s^{-1}.

3.3. Optimization of experimental conditions

The effect of buffer pH on the behavior of the immunosensor was investigated over a pH range from 5.0 to 8.5 with 50 ng mL^{-1} CEA. As shown in Fig. 6A, the current response increased from pH 5.0, reached the maximum value at pH 6.5, and then decreased to pH 8.5. It was known that the stability of CS solution were pH dependent and strong acidic medium could decrease the stability of CS [21,23]. In addition, highly acidic or alkaline solution would damage the bioactivity of immobilized proteins. Hence, pH 6.5 was chosen as the optimal pH of the detection solution to obtain a high sensitivity.

The effect of incubation time was investigated in the time range of 0–25 min with 50 ng mL^{-1} CEA. The results showed that ΔI rapidly increased within the first 15 min and then tended to level off (Fig. 6B) because of the saturated formation of immunocomplex. Therefore, 20 min was chosen as the optimal incubation time.

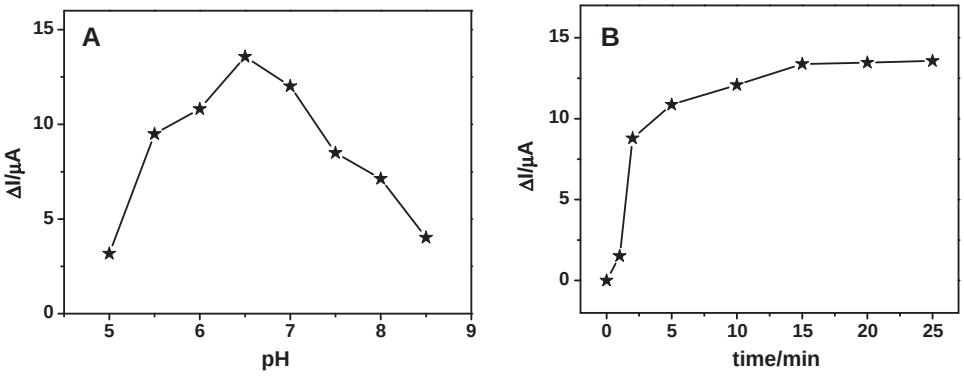

Fig. 6. Influence of the (A) pH of the PBS and (B) incubation time on the immunosensor.

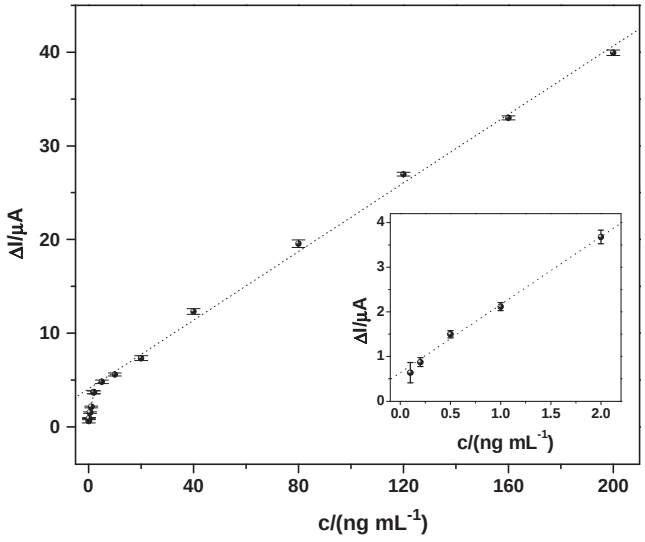

Fig. 7. Calibration plot of the change of reduction current response of the immunosensor versus concentration of CEA under optimal conditions. Inset: linear relationship between the change of reduction current response and concentration of CEA in the ranges of 0.1–2.0 ng mL^{-1}. Scan rate 50 mV s^{-1}.

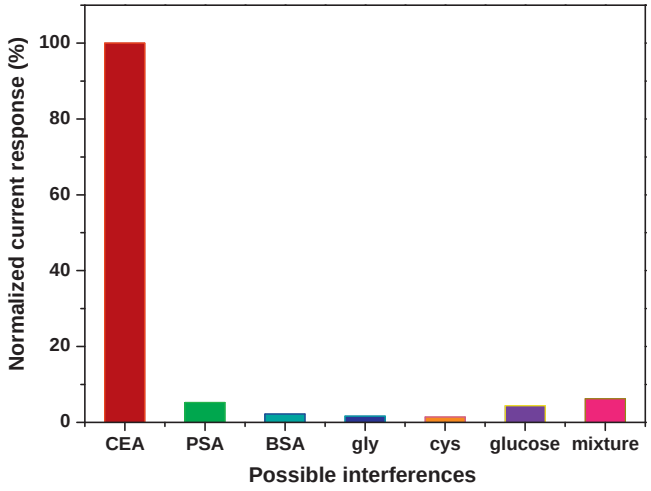

Fig. 8. Selectivity of the immunosensor in the presence of CEA (50 ng mL^{-1}), prostate specific antigen (50 ng mL^{-1}), bovine serum albumin (50 ng mL^{-1}), glycine (2 μg mL^{-1}), cysteine (2 μg mL^{-1}), glucose (1 mg mL^{-1}) and mixture containing all the interferences stated above.

3.4. Calibration curve of the immunosensor

The calibration curve for the detection of CEA was obtained by using the prepared immunosensor under optimal experimental conditions (Fig. 7). When antigens had bound with the antibodies immobilized on the electrode, the antigen–antibody complexes coating on the surface of the electrode inhibited the electron transfer. The change of reduction peak current response (ΔI) of the immunosensor was found to be proportional to the CEA concentration in two linear ranges from 0.1 to 2.0 ng mL^{-1} and from 2.0 to 200.0 ng mL^{-1}, with a detection limit of 0.04 ng mL^{-1} (S/N = 3). The linear slopes were 1.56 and 0.18 μA mL ng^{-1}, and the correlation coefficients were 0.997 and 0.999, respectively. The calibration curve presented two slopes, probably, because the amount of antibody immobilized on the electrode surface was some certain. When the antigen concentration increased, active sites of antibody immobilized on the electrode surface became fewer and led to a decrease of sensitivity [36]. The analytical performance of the proposed immunosensor had been compared with the CEA immunosensors reported previously. The comparative data (Table 1) suggested the proposed immunosensor had a lower detection limit and a wider linear range.

3.5. Selectivity of the immunosensor

In this study, some potential interferences, including prostate specific antigen (50 ng mL^{-1}), bovine serum albumin (50 ng mL^{-1}), cysteine (2 μg mL^{-1}), glycine (2 μg mL^{-1}), glucose (1 mg mL^{-1}) and mixture, were used to evaluate the selectivity of the immunosensor. The results (Fig. 8) showed that the interferences of relatively high concentrations did not affect the detection obviously. Thus the proposed immunosensor based on the high specific antigen–antibody reaction had an acceptable selectivity.

3.6. Regeneration of the immunosensor

Regeneration is an important factor in the application of immunosensors. The prepared immunosensor could be regenerated by simply treating with regeneration solutions for about 5 min to dissociate the antibody–antigen complex. The relative standard deviations (R.S.D.) of 3.8% for 4 M urea solution and 3.4% for 0.2 M glycine–hydrochloric acid (Gly–HCl) solution (pH 2.8) were obtained when the immunosensor was used for five regenerations and measurements at CEA concentrations of 50 ng mL^{-1}.

3.7. Reproducibility and stability of the immunosensor

The reproducibility of the immunosensor was estimated by intra-assay and inter-assay coefficients of variation (CVs). The intra-assay precision was evaluated by assaying the CEA level for five determinations of one sample on the same immunosensor. The intra-assay CVs of this method were 3.5% and 3.2% at CEA concentrations of 20 and 50 ng mL^{-1}, respectively. The inter-assay precision was evaluated by determining the CEA level in one sample with five immunosensors. The inter-assay CV was 3.7% at the CEA concentration of 50 ng mL^{-1}, showing an acceptable reproducibility.

The long-term stability of immunosensor was investigated over a 30-day period, stored at 4 °C. The current response to 50 ng mL^{-1} CEA maintained about 97.1%, 94.4% and 90.5% of the original value after the storage periods of 10 days, 20 days and 30 days, respectively. The good stability may be attributed to the fact that the CS–CNTs–GNPs film could provide a biocompatible microenvironment for the biomolecules immobilization.

Table 1
Comparison of different immunosensors for detection of CEA.

Detection methods	Linear range (ng mL^{-1})	Detection limit (ng mL^{-1})	Reference
Cyclic voltammetry	0.2–120	0.06	[37]
Cyclic voltammetry	0.25–8.0 and 8.0–100	0.08	[38]
Cyclic voltammetry	0.2–10.0 and 10.0–160	0.08	[26]
Differential pulse voltammetry	0.3–2.5 and 2.5–20.0	0.01	[39]
Cyclic voltammetry	0.1–2.0 and 2.0–200	0.04	This work

Table 2
Comparison of serum CEA levels determined using two methods.

Serum samples	1	2	3	4	5
Immunosensor ($ng\,mL^{-1}$)	1.46	2.72	10.23	42.61	62.09
ELISA ($ng\,mL^{-1}$)	1.58	2.95	9.60	40.60	59.40
Relative deviation (%)	−7.59	−7.80	6.56	4.95	4.53

3.8. Preliminary application of the immunosensor

To demonstrate the possible clinical application of the proposed method, human serum samples were assayed by the prepared immunosensor and ELISA. The results were listed in Table 2. The relative deviation between the two methods was in the range of −7.80 to 4.53%, which indicated that the two methods were in acceptable agreement. Thus, the proposed immunosensor could be further applied to clinical detection of CEA.

4. Conclusion

In this work, a novel strategy for construction of immunosensor was developed based on immobilization of anti-CEA on the electrode modified with CS–CNTs–GNPs nanocomposite film. The CS–CNTs–GNPs nanocomposite film obtained via the one-step electrodeposition method showed a porous three-dimensional morphology, exhibited improved conductivity and high stability due to the introduction of CNTs and GNPs, and offered a large specific surface area and a biocompatible microenvironment for the immobilization of antibodies with fine bioactivity. Therefore, the proposed immunosensor presented some advantages, including a simple and controllable fabrication process, high sensitivity, low detection limit, satisfactory reproducibility, long-term storage stability, and cost-effectiveness. The proposed immunosensor could provide a new approach to detection in clinical diagnosis.

Acknowledgements

This research was supported by the National Natural Science Foundation of China (Nos. 30800247 and 20805043).

References

[1] L.N. Wu, F. Yan, H.X. Ju, J. Immunol. Methods 322 (2007) 12–19.
[2] S. Centi, S. Laschi, M. Mascini, Talanta 73 (2007) 394–399.
[3] J. Zhang, J.P. Lei, C.L. Xu, L. Ding, H.X. Ju, Anal. Chem. 82 (2010) 1117–1122.
[4] R. Malhotra, V. Patel, J.P. Vaqué, J.S. Gutkind, J.F. Rusling, Anal. Chem. 82 (2010) 3118–3123.
[5] W.Z. Jia, K. Wang, Z.J. Zhu, H.T. Song, X.H. Xia, Langmuir 23 (2007) 11896–11900.
[6] M.G. Zhang, A. Smith, W. Gorski, Anal. Chem. 76 (2004) 5045–5050.
[7] Y.J. Zou, C.L. Xiang, L.X. Sun, F. Xu, Biosens. Bioelectron. 23 (2008) 1010–1016.
[8] J. Chen, F. Yan, D. Du, J. Wu, H.X. Ju, Electroanalysis 18 (2006) 670–676.
[9] F. Li, W. Chen, C.F. Tang, S.S. Zhang, Talanta 77 (2009) 1304–1308.
[10] L. Tan, Y.Q. Chen, H. Yang, Y. Shi, J.F. Si, G.M. Yang, Z.S. Wu, P. Wang, X.X. Lu, H.P. Bai, Y.H. Yang, Sens. Actuators B: Chem. 142 (2009) 316–320.
[11] J.H. Lin, C.Y. He, L.J. Zhang, S.S. Zhang, Anal. Biochem. 384 (2009) 130–135.
[12] H. Yi, L.Q. Wu, R. Ghodssi, G.W. Rubloff, G.F. Payne, W.E. Bentley, Anal. Chem. 76 (2004) 365–372.
[13] F.N. Xi, L.J. Liu, Z.C. Chen, X.F. Lin, Talanta 78 (2009) 1077–1082.
[14] Y.C. Zhang, C. Ji, Anal. Chem. 82 (2010) 5275–5281.
[15] R. Fernandes, L.Q. Wu, T.H. Chen, H.M. Yi, G.W. Rubloff, R. Ghodssi, W.E. Bentley, G.F. Payne, Langmuir 19 (2003) 4058–4062.
[16] Y. Du, X.L. Luo, J.J. Xu, H.Y. Chen, Bioelectrochemistry 70 (2007) 342–347.
[17] L.Q. Wu, K. Lee, X. Wang, D.S. English, W. Losert, G.F. Payne, Langmuir 21 (2005) 3641–3646.
[18] X.L. Luo, J.J. Xu, J.L. Wang, H.Y. Chen, Chem. Commun. 216 (2005) 9–2171.
[19] F.N. Xi, L.J. Liu, Q. Wu, X.F. Lin, Biosens. Bioelectron. 24 (2008) 29–34.
[20] D. Feng, F. Wang, Z.L. Chen, Sens. Actuators B: Chem. 138 (2009) 539–544.
[21] J.D. Qiu, R. Wang, R.P. Liang, X.H. Xia, Biosens. Bioelectron. 24 (2009) 2920–2925.
[22] M. Diaconu, S.C. Litescu, G.L. Radu, Sens. Actuators B: Chem. 145 (2010) 800–806.
[23] J.D. Qiu, R.P. Liang, R. Wang, L.X. Fan, Y.W. Chen, X.H. Xia, Biosens. Bioelectron. 25 (2009) 852–857.
[24] R.P. Liang, L.X. Fan, D.M. Huang, J.D. Qiu, Electroanalysis 23 (2011) 719–727.
[25] Y.X. Liu, R. Yuan, Y.Q. Chai, C.L. Hong, S. Guan, Bioprocess. Biosyst. Eng. 33 (2010) 613–618.
[26] Y.X. Liu, R. Yuan, Y.Q. Chai, C. Hong, K.G. Liu, S. Guan, Microchim. Acta 167 (2009) 217–224.
[27] H.C. Yang, R. Yuan, Y.Q. Chai, Y. Zhuo, Colloid Surf. B: Biointerfaces 82 (2011) 463–469.
[28] J.A.A. Ho, Y.C. Lin, L.S. Wang, K.C. Hwang, P.T. Chou, Anal. Chem. 81 (2009) 1340–1346.
[29] M.Y. Liu, C.P. Jia, Q.H. Jin, X.H. Lou, S.H. Yao, J.Q. Xiang, J.L. Zhao, Talanta 81 (2010) 1625–1629.
[30] L. Qian, X.R. Yang, Talanta 68 (2006) 721–727.
[31] L.J. Liu, F. Zhang, F.N. Xi, Z.C. Chen, X.F. Lin, J. Electroanal. Chem. 623 (2008) 135–141.
[32] K.C. Grabar, R.G. Freeman, M.B. Hommer, M.J. Natan, Anal. Chem. 67 (1995) 735–743.
[33] Z.J. Song, R. Yuan, Y.Q. Chai, B. Yin, P. Fu, J.F. Wang, Electrochim. Acta 55 (2010) 1778–1784.
[34] X.Q. Ran, R. Yuan, Y.Q. Chai, C.L. Hong, X.Q. Qian, Colloid Surf. B: Biointerfaces 79 (2010) 421–426.
[35] M.M. Gu, J.J. Zhang, Y. Li, L.P. Jiang, J.J. Zhu, Talanta 80 (2009) 246–249.
[36] Y.R. Yuan, R. Yuan, Y.Q. Chai, Y. Zhuo, X.M. Miao, J. Electroanal. Chem. 626 (2009) 6–13.
[37] X.L. He, R. Yuan, Y.Q. Chai, Y.T. Shi, J. Biochem. Biophys. Methods 70 (2008) 823–829.
[38] S.J. Ling, R. Yuan, Y.Q. Chai, T.T. Zhang, Bioprocess. Biosyst. Eng. 32 (2009) 407–414.
[39] K.J. Huang, D.J. Niu, W.Z. Xie, W. Wang, Anal. Chim. Acta 659 (2010) 102–108.